Supramolecular Chemistry

DOI: 10.1002/ange.201306510

Silver-Mediated Formation of a Cofacial Porphyrin Dimer with the Ability to Intercalate Aromatic Molecules**

*Takashi Nakamura, Hitoshi Ube, and Mitsuhiko Shionoya**

Porphyrins are widely used for functional molecular systems based on their excellent photophysical and redox properties.[1] In particular, multiple porphyrins arranged in a well-ordered manner show unique functions such as photoelectron conversion, catalysis, and molecular recognition, all of which cannot be achieved by a monomeric porphyrin analogue.[2,3] Cofacial porphyrin dimers can be readily constructed by linking two porphyrin rings by covalent,[4–12] hydrogen,[13] or coordination bonds.[14–19] So far, a great number of porphyrin dimers have been reported as host molecules for guest recognition. For example, a fullerene molecule is captured by π–π interactions,[6,9,15] or various ligand molecules bind to the axial site of the central metals from inside.[5,13,16,17,19]

When two aromatic rings are positioned parallel to each other at a distance of about 6–7 Å, the dimer can be a good receptor for intercalating guest molecules through π–π interactions. Many cofacial dimers of porphyrins[8,10–12,18] and other aromatic compounds[18,20–23] have been developed for their recognition of aromatic guests. However, many aromatic-dimer host molecules either have low-binding ability because of the structural flexibility (e.g., rotation of aromatic moieties) or are difficult to synthesize (e.g., inefficient linking or cyclization).

Coordination-driven self-assembly of organic ligands and metal ions is an efficient way to construct three-dimensional molecular architectures.[24–27] Multiporphyrin supramolecular structures made up of metal ions and porphyrin ligands equipped with multiple coordination sites have been widely investigated to explore their unique molecular functions.[3,14–19,28–34] We previously reported the tetrakis(bpy) Zn-porphyrin **1** (bpy = 2,2′-bipyridin-5-yl, see Scheme 1) as a building block for coordination-driven self-assembled systems, and found that complexation of Zn^{II} ions and **1** in a water-containing organic solvent produced the cage complex $[Zn_{11}\mathbf{1}_6(H_2O)_{18}]^{22+}$.[35] The cage complex was composed of tris(bpy) Zn^{II} units and hydrated bis(bpy) Zn^{II} units, which adopted six-coordinate octahedral geometries. In the study, the crystal structure of **1** revealed that the bpy groups did not have a coplanar conformation with the central porphyrin ring because of the steric repulsion between their hydrogen atoms. Considering the structural limitation of this ligand, we envisioned that complexation of the bpy groups of **1** with metal ions, which can adopt a four-coordinate, square-planar coordination geometry, would form a dimeric complex in which two porphyrin rings are arranged face to face. Here, Ag^I was selected as a key element for coordination-driven self-assembly. The Ag^I ion is coordinatively labile and therefore rapidly provides thermodynamically-stable, self-assembled products. In addition, Ag^I is geometrically flexible in coordination structures, and the four-coordinate, square-planar geometry is dominant under certain conditions.[36,37] Several square-planar Ag^I complexes, wherein two *N*-*N* bidentate diimine ligands face each other, have been reported so far.[38–41]

Herein, we report the construction of the cofacial porphyrin dimer $[Ag_4\mathbf{1}_2]^{4+}$ ($\mathbf{2}^{4+}$) by simple and quantitative coordination-driven self-assembly of two components, Ag^I and **1** (Scheme 1). In the dimeric structure of $\mathbf{2}^{4+}$, four bis(bpy) Ag^I units are directly attached to every meso position of the porphyrin rings, thus setting the two porphyrin rings parallel to each other and making the whole framework rigid. The distance between the two porphyrins was ideal for intercalation of aromatic molecules. With these features, $\mathbf{2}^{4+}$ worked as an excellent receptor for binding aromatic guest molecules with high selectivity. Notably, $\mathbf{2}^{4+}$ showed a high

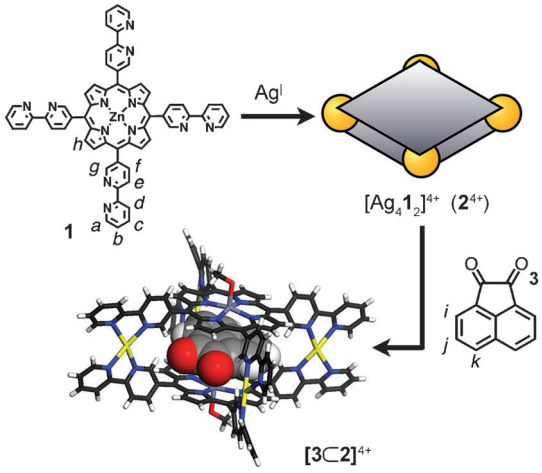

Scheme 1. Silver-mediated formation of a cofacial porphyrin dimer $[Ag_4\mathbf{1}_2]^{4+}$ ($\mathbf{2}^{4+}$) and the intercalation of an acenaphthenequinone (**3**) molecule between the two porphyrin rings of $\mathbf{2}^{4+}$.

[*] Dr. T. Nakamura, Dr. H. Ube, Prof. Dr. M. Shionoya
Department of Chemistry, Graduate School of Science
The University of Tokyo
7-3-1 Hongo, Bunkyo-ku, Tokyo 113-0033 (Japan)
E-mail: shionoya@chem.s.u-tokyo.ac.jp
Homepage: http://www.chem.s.u-tokyo.ac.jp/users/bioinorg/indexE.html

[**] We thank Dr. Ryosuke Miyake of Ochanomizu University for helpful discussions on single-crystal X-ray diffraction analysis. This research was supported by the Global COE Program and KAKENHI from the Japan Society for the Promotion of Science (JSPS) and MEXT (Japan). T.N. thanks JSPS Research Fellowship for Young Scientists.

Supporting information for this article is available on the WWW under http://dx.doi.org/10.1002/anie.201306510.

intercalation ability for acenaphthenequinone (**3**), intercalation which results from efficient π–π interactions with the Zn-porphyrins and from multiple hydrogen bonds between the pyridyl C–H bonds of $\mathbf{2}^{4+}$ and the carbonyl oxygen atoms of **3**.

The complexation of **1** and AgOTf ($OTf^- = CF_3SO_3^-$) was investigated by ^{1}H NMR spectroscopy using a mixed solvent, $CDCl_3/CD_3OD = 1:1$ (v/v) (Figure 1 and see Figure S5 in the Supporting Information). The solvent was chosen for the

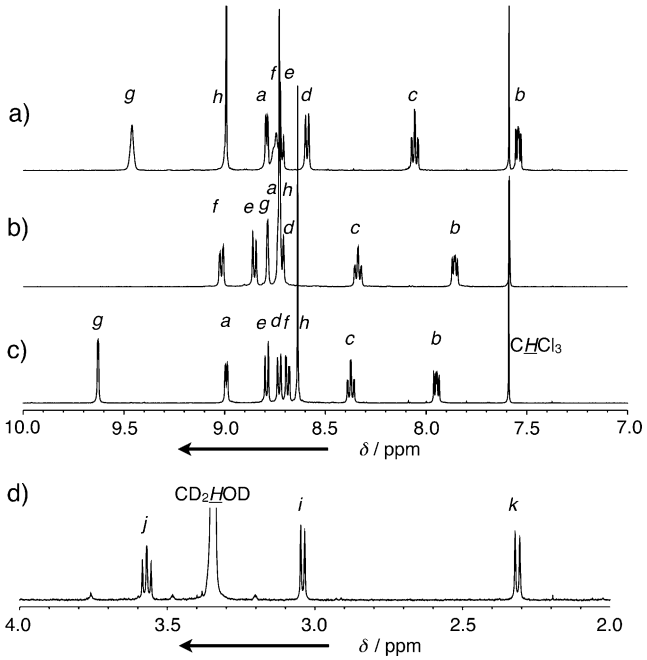

Figure 1. Formation of the porphyrin dimer $[Ag_4\mathbf{1}_2]^{4+}$ ($\mathbf{2}^{4+}$) and an inclusion complex $[\mathbf{3}\subset\mathbf{2}]^{4+}$. ^{1}H NMR spectra of **1**, $\mathbf{2}\cdot(OTf)_4$, and $[\mathbf{3}\subset\mathbf{2}](OTf)_4$ ($CDCl_3/CD_3OD = 1:1$ (v/v), 500 MHz, 300 K). See the chemical formula in Scheme 1 for the assignment of the ^{1}H signals. a) **1**. b) $\mathbf{2}^{4+}$ constructed from **1** and AgOTf (2 equiv [/**1**]). c,d) Inclusion complex $[\mathbf{3}\subset\mathbf{2}]^{4+}$.

good solubility of both **1** and the complexes. Upon addition of AgOTf to a solution of **1**, a set of sharp NMR signals was observed when the ratio of **1** to Ag^I reached 1:2, thus indicating the quantitative formation of a new single species (Figure 1 b). The ^{1}H NMR spectrum showed that **1** adopted a C_4 symmetry in the complex. The metal to ligand ratio (**1**/$Ag^I = 1:2$) suggested that all four bpy groups of **1** form bis(bpy) Ag^I units. ESI-MS measurements of the sample gave a set of signals assigned to the porphyrin dimer $[Ag_4\mathbf{1}_2](OTf)_4$ [$\mathbf{2}\cdot(OTf)_4$] (Figure S6).

In a control experiment, the complexation behavior of 2,2′-bipyridine and AgOTf was investigated by ^{1}H NMR spectroscopy under the same reaction conditions (Figure S7). In this case, however, the bis(bpy) Ag^I complex was not formed quantitatively when the ratio of bpy to Ag^I was 2:1. This result shows that the way in which the four bpy groups are situated on the rigid ligand framework was important for the cooperative formation of $\mathbf{2}^{4+}$. The dimer $\mathbf{2}^{4+}$ was also constructed using Ag^I salts with different counter anions, namely, BF_4^-, $CF_3CO_2^-$, $CH_3SO_3^-$, and NO_3^- (see Figure S8). The ^{1}H NMR spectra of these complexes in $CDCl_3/CD_3OD = 1:1$ (v/v) were very similar to each other, and suggests that the solution structure of $\mathbf{2}^{4+}$ was essentially identical, regardless of the counter anions.

Next, guest intercalation between two porphyrin rings of $\mathbf{2}^{4+}$ was investigated. Acenaphthenequinone (**3**), a π-electron-deficient aromatic molecule, was firstly chosen as a guest molecule with the anticipation of π–π interactions between the guest and the π-electron-rich Zn-porphyrin rings. Upon the addition of **3** to the porphyrin dimer $\mathbf{2}\cdot(OTf)_4$ in $CDCl_3/CD_3OD = 1:1$, an inclusion complex $[\mathbf{3}\subset\mathbf{2}](OTf)_4$ was quantitatively formed as observed in the ^{1}H NMR spectrum (Figure 1 c,d). In–out guest exchange of **3** was slower than the ^{1}H NMR timescale at 300 K. ^{1}H NMR signals of the intercalated **3** of $[\mathbf{3}\subset\mathbf{2}](OTf)_4$ were observed at $\delta = 3.57$, 3.04, and 2.31 ppm, which were significantly upfield shifted ($\Delta\delta = -4.35$ to -6.06 ppm) compared to those in the absence of $\mathbf{2}^{4+}$. This result indicates that the protons of the intercalated **3** were positioned between the two Zn-porphyrin rings of $\mathbf{2}^{4+}$ and therefore remarkably affected by the shielding effect. The binding of **3** within $\mathbf{2}^{4+}$ was confirmed by ^{1}H-^{1}H NOESY NMR spectroscopy (Figure S11), in which NOE (nuclear Overhauser effect) cross-peaks were observed between the protons (*i*, *j*, *k*) of **3** and the proton (*g*) of $\mathbf{2}^{4+}$. ^{1}H DOSY (diffusion-ordered spectroscopy) measurements gave the same diffusion coefficient for ^{1}H signals of $\mathbf{2}^{4+}$ and **3**, and supports the formation of an inclusion complex $[\mathbf{3}\subset\mathbf{2}]^{4+}$ (Figure S12). ESI-MS measurements of the sample also confirmed the formation of the inclusion complex $[\mathbf{3}\subset\mathbf{2}](OTf)_4$ (Figure S13). In synthetic-scale experiments, $[\mathbf{3}\subset\mathbf{2}]^{4+}$ complexes with different counter anions were prepared almost quantitatively after recrystallization by diffusion of Et_2O vapor into $CHCl_3/CH_3OH = 1:1$ solutions of $[\mathbf{3}\subset\mathbf{2}]^{4+}$ salts.

Crystals suitable for X-ray diffraction analysis were obtained by slow diffusion of Et_2O vapor into a CH_3OH solution of the inclusion complex $[\mathbf{3}\subset\mathbf{2}](CF_3CO_2)_4$. The single-crystal X-ray diffraction analysis clearly revealed the structure of the inclusion complex $[\mathbf{3}\subset\mathbf{2}]^{4+}$ (Figure 2). As expected, one acenaphthenequinone molecule was intercalated between two parallel Zn-porphyrin rings linked by four bis(bpy) Ag^I units (Figure 2 a,b). There are two kinds of bis(bpy) Ag^I units for $[\mathbf{3}\subset\mathbf{2}](CF_3CO_2)_4$ in the crystal (Figure 2 c,d). Both Ag^I centers can be described as four-coordinate distorted square-planar geometries, since *trans* N-Ag-N angles were in the range of 153–172°. In solution, all bis(bpy) Ag^I units are equivalent on the NMR timescale (Figure 1 c). The interplane distance between the Zn-porphyrin ring and the included guest was about 3.1–3.2 Å, which suggests strong π–π interactions. The two carbonyl groups of **3** were found to point towards an opening in the dimer $\mathbf{2}^{4+}$. And this orientation can be explained by the stabilization resulting from multiple hydrogen bonds between the C–H of the pyridyl groups (proton *g* in Scheme 1) of $\mathbf{2}^{4+}$ and the carbonyl oxygen atoms of **3** (C–H···O distance; 3.2–3.4 Å) (Figure 2 e). The Zn-porphyrin was bound by one axial CH_3OH ligand to form a square-pyramidal geometry. In the packing structure, several intermolecular hydrogen bonds including the C–H of the pyridyl groups were found between neighboring $[\mathbf{3}\subset\mathbf{2}]^{4+}$

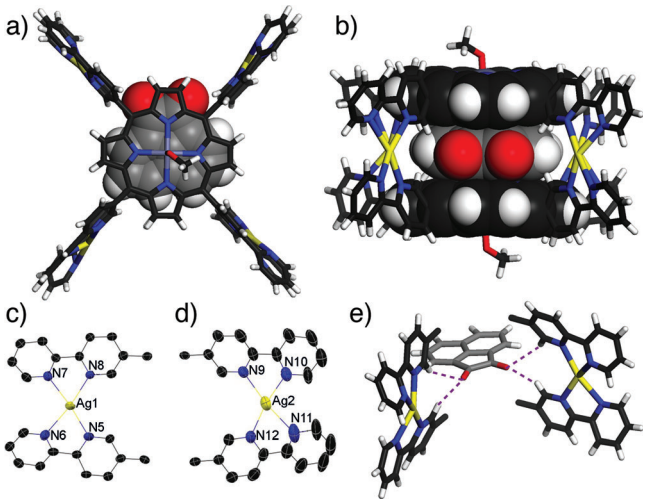

Figure 2. The X-ray crystal structure of $[\mathbf{3}\subset(\mathbf{2})(CH_3OH)_2]\cdot(CF_3CO_2)_4$. $CF_3CO_2^-$ anions and hydrogen atoms of CH_3OH coordinating to Zn^{II} are omitted for clarity. Ag yellow, Zn light purple, C black (for $\mathbf{2}^{4+}$ and CH_3OH), C gray (for **3**), N blue, O red, H white. **3** (a) as well as **3** and the porphyrin rings (b) are shown as a space-filling model. The structures in c) and d) are shown in an ellipsoidal model. The others are shown as a stick model. Top view (a) and side view (b) of $[\mathbf{3}\subset(\mathbf{2})(CH_3OH)_2]^{4+}$. c,d) Bis(bpy) Ag^I units, in which Ag^I centers adopted a four-coordinate distorted square-planar geometry. Thermal ellipsoids are set at 50% probability. Hydrogen atoms are omitted for clarity. See the Experimental Section for selected bond lengths and angles. e) Hydrogen bonds (purple dashed line) between C–H bonds of pyridyl groups in $\mathbf{2}^{4+}$ and carbonyl oxygen atoms of **3**.

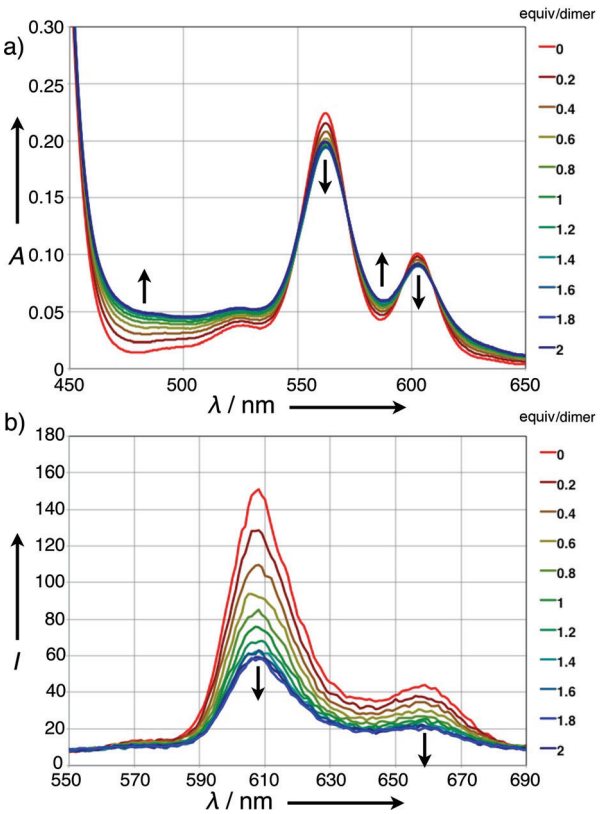

Figure 3. UV/Vis absorption and emission spectra upon titration of 1,4-naphthoquinone (**4**) with the porphyrin dimer $\mathbf{2}\cdot(OTf)_4$ ($[\mathbf{2}^{4+}] = 5.0\ \mu M$, $CHCl_3/CH_3OH = 1{:}1$ (v/v), $\lambda = 1.0$ cm, 300 K). 2.5 equiv of AgOTf was added to **1** to ensure the complete formation of $\mathbf{2}^{4+}$ at this concentration (for the formation of dimer $\mathbf{2}\cdot(OTf)_4$, see Figure S9). a) UV/Vis absorption spectra. b) Emission spectra (excitation wavelength; $\lambda = 360$ nm).

molecules, and thus two-dimensional interconnected channel structures were formed along the *a* axis and *b* axis (Figure S15).

Next, the binding behavior of aromatic guests to $\mathbf{2}^{4+}$ was investigated by guest titration experiments using UV/Vis absorption and emission spectroscopy. The experimental results using 1,4-naphthoquinone (**4**) and $\mathbf{2}^{4+}$ in a mixed solvent $CHCl_3/CH_3OH = 1{:}1$ are shown in Figure 3. Absorbance arising from $\mathbf{2}^{4+}$ changed with isosbestic points during the titration, and indicates the formation of the inclusion complex $[\mathbf{4}\subset\mathbf{2}](OTf)_4$ (Figure 3a). The fluorescence intensity of the Zn-porphyrin units was reduced upon the addition of **4**, and suggests photoinduced electron transfer from the Zn-porphyrin to **4** (Figure 3b). The binding constant, K_a, of the guest G to $\mathbf{2}^{4+}$ is defined by Equation (1).

$$K_a = \frac{[G \subset 2^{4+}]}{[G][2^{4+}]} \quad [M^{-1}] \qquad (1)$$

From the changes in absorbance at $\lambda = 586$ nm, the binding constant K_a of **4** with $\mathbf{2}^{4+}$ was determined to be $\log K_a = 6.5$ ($CHCl_3/CH_3OH = 1{:}1$, 300 K; Figure S16).

Binding constants of other aromatic guests were determined similarly by titration experiments using ^1H NMR and UV/Vis spectroscopy as summarized in Table 1. The porphyrin dimer $\mathbf{2}^{4+}$ shows high selectivity towards these guest molecules. The selectivity in guest inclusion can be explained by the following two points: 1) π-electron-deficient guests interact with a π-electron-rich Zn-porphyrin more strongly (**3** and **4** versus **8** and **9**); 2) guests comparable in size to substituted naphthalenes are suitable for intercalation within the cavity of $\mathbf{2}^{4+}$ (**3**–**5** versus **6** and **7**). Remarkably, the binding constant of **3** was too high to evaluate by UV/Vis titration measurements, and was therefore determined by a guest competition experiment using **4** (Figure S19). The exceptionally high affinity of **3** ($\log K_a = 8.1$) for $\mathbf{2}^{4+}$ is attributed to: 1) the electron-deficient π surface of **3**, 2) the suitable size of **3** for intercalation, and more importantly, 3) multipoint hydrogen bonding between the pyridine C–H of $\mathbf{2}^{4+}$ and the carbonyl O atoms of **3**, as revealed by X-ray crystal analysis (Figure 2e).

In conclusion, the novel dimeric complex $\mathbf{2}^{4+}$ was synthesized by a one-pot and quantitative self-assembly of **1** and Ag^I ions. In the structure of $\mathbf{2}^{4+}$, two parallel Zn-porphyrin rings are rigidly preorganized by four bis(bpy) Ag^I units. The distance between two Zn-porphyrin rings of $\mathbf{2}^{4+}$ is ideal for intercalation of aromatic molecules, and indeed $\mathbf{2}^{4+}$ served as a selective and effective receptor for π-electron-deficient guests. Notably, $\mathbf{2}^{4+}$ exhibited a remarkably high intercalation ability towards **3** owing to the strong π–π interactions and the multipoint hydrogen bonding. This dimeric sandwich motif deserves further investigations on unique photochemical, redox, and catalytic properties.

Table 1: Binding constants, K_a [M^{-1}], of aromatic guests with the porphyrin dimer **2**·$(OTf)_4$.

Compounds	Structures	log K_a[a]	Method[b]
3	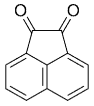	8.1[c]	C
5	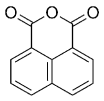	7.6	C
4	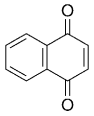	6.5	A
6	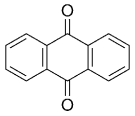	3.6	B
7	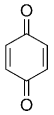	3.0	B
8	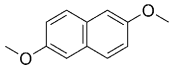	2.5	B
9		1.7	B
10	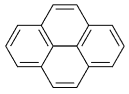	< 1	B

[a] $CHCl_3/CH_3OH$ or $CDCl_3/CD_3OD$ = 1:1 (v/v), 300 K. [b] Method A: UV/Vis titration ([**2**·$(OTf)_4$] = 5.0 μM). Method B: ^{1}H NMR titration ([**2**·$(OTf)_4$] = 1 mM). Method C: Competitive ^{1}H NMR titration in the presence of 100 equiv [/$\mathbf{2}^{4+}$] of **4** ([**2**·$(OTf)_4$] = 1 mM). [c] In $CDCl_3/CD_3OD$ = 1:1. **3** was in equilibrium with its methyl hemiketal form, 2-hydroxy-2-methoxyacenaphthylen-1(2*H*)-one (**11**). At 300 K, the equilibrium was achieved within 5 minutes and the ratio was **3**/**11** = 4:1. See the Supporting Information for the details.

Experimental Section

Crystals suitable for X-ray analysis were obtained by slow vapor diffusion of Et_2O into a CH_3OH solution of [**3**⊂**2**]$(CF_3CO_2)_4$ at room temperature in the dark. Crystal data for [**3**⊂(**2**)$(CH_3OH)_2$]-$(CF_3CO_2)_4$: $C_{142}H_{86}Ag_4F_{12}N_{24}O_{12}Zn_2$, $Fw = 3110.61$, red blocks, $0.22 \times 0.20 \times 0.10$ mm^3, triclinic, space group $P\bar{1}$ (#2), $a = 13.7356(7)$, $b = 17.1048(9)$, $c = 18.0872(8)$ Å, $\alpha = 80.591(2)$, $\beta = 76.037(2)$, $\gamma = 72.554(2)°$, $V = 3915.1(4)$ Å^3, $Z = 1$, $T = 93$ K, $\lambda(Mo_{K\alpha}) = 0.71075$ Å, $2\theta_{max} = 55.0°$, $R_1 = 0.0728$, $wR_2 = 0.2608$ (after SQUEEZE), GOF = 1.049, largest diff. peak and hole 1.37/−1.66 e$^-$ Å^{-3}. See the Supporting Information for refinement details. Selected bond lengths [Å]: Ag1–N5 2.306(6), Ag1–N6 2.429(5), Ag1–N7 2.369(5), Ag1–N8 2.338(5), Ag2–N9 2.395(6), Ag2–N10 2.328(8), Ag2–N11 2.527(8), Ag2–N12 2.282(8). Selected bond angles [°]; N5-Ag1-N6 71.98(17), N5-Ag1-N7 154.9(2), N5-Ag1-N8 118.33(16), N6-Ag1-N7 101.33(16), N6-Ag1-N8 167.71(18), N7-Ag1-N8 72.15(16), N9-Ag2-N10 70.8(2), N9-Ag2-N11 171.6(3), N9-Ag2-N12 120.0(2), N10-Ag2-N11 102.4(3), N10-Ag2-N12 153.42(19), N11-Ag2-N12 68.2(3). CCDC 937862 contains the supplementary crystallographic data for this paper. These data can be obtained free of charge from The Cambridge Crystallographic Data Centre via www.ccdc.cam.ac.uk/data_request/cif.

Received: July 26, 2013
Published online: September 24, 2013

Keywords: host-guest systems · intercalations · porphyrinoids · silver · supramolecular chemistry

[1] K. M. Kadish, K. M. Smith, R. Guilard, *Handbook of Porphyrin Science*, Vol. 1–25, World Scientific, Singapore, **2010–2012**.
[2] D. Kim, *Multiporphyrin Arrays: Fundamentals and Applications*, Pan Stanford Publishing, Singapore, **2012**.
[3] I. Beletskaya, V. S. Tyurin, A. Y. Tsivadze, R. Guilard, C. Stern, *Chem. Rev.* **2009**, *109*, 1659–1713.
[4] C. K. Chang, I. Abdalmuhdi, *Angew. Chem.* **1984**, *96*, 154–155; *Angew. Chem. Int. Ed. Engl.* **1984**, *23*, 164–165.
[5] S. Anderson, H. L. Anderson, J. K. M. Sanders, *J. Chem. Soc. Perkin Trans. 1* **1995**, 2247–2254.
[6] K. Tashiro, T. Aida, J.-Yu. Zheng, K. Kinbara, K. Saigo, S. Sakamoto, K. Yamaguchi, *J. Am. Chem. Soc.* **1999**, *121*, 9477–9478.
[7] A. Ohashi, A. Satake, Y. Kobuke, *Bull. Chem. Soc. Jpn.* **2004**, *77*, 365–374.
[8] M. Tanaka, K. Ohkubo, C. P. Gros, R. Guilard, S. Fukuzumi, *J. Am. Chem. Soc.* **2006**, *128*, 14625–14633.
[9] H. Nobukuni, Y. Shimazaki, F. Tani, Y. Naruta, *Angew. Chem.* **2007**, *119*, 9133–9136; *Angew. Chem. Int. Ed.* **2007**, *46*, 8975–8978.
[10] T. Ema, N. Ura, K. Eguchi, Y. Ise, T. Sakai, *Chem. Commun.* **2011**, *47*, 6090–6092.
[11] A. Chaudhary, S. P. Rath, *Chem. Eur. J.* **2012**, *18*, 7404–7417.
[12] S. Yamamoto, H. Iida, E. Yashima, *Angew. Chem.* **2013**, *125*, 6987–6991; *Angew. Chem. Int. Ed.* **2013**, *52*, 6849–6853.
[13] Y. Kuroda, A. Kawashima, Y. Hayashi, H. Ogoshi, *J. Am. Chem. Soc.* **1997**, *119*, 4929–4933.
[14] V. Thanabal, V. Krishnan, *J. Am. Chem. Soc.* **1982**, *104*, 3643–3650.
[15] D. Sun, F. S. Tham, C. A. Reed, L. Chaker, M. Burgess, W. Boyd, *J. Am. Chem. Soc.* **2000**, *122*, 10704–10705.
[16] A. Ikeda, M. Ayabe, S. Shinkai, S. Sakamoto, K. Yamaguchi, *Org. Lett.* **2000**, *2*, 3707–3710.
[17] R. S. K. Kishore, T. Paululat, T. Schmittel, *Chem. Eur. J.* **2006**, *12*, 8136–8149.
[18] Y.-R. Zheng, Z. Zhao, M. Wang, K. Ghosh, J. B. Pollock, T. R. Cook, P. J. Stang, *J. Am. Chem. Soc.* **2010**, *132*, 16873–16882.
[19] E. N. Kirichenko, V. S. Tyurin, I. P. Beletskaya, *Prot. Met. Phys. Chem. Surf.* **2011**, *47*, 424–434.
[20] C. A. Hunter, K. R. Lawson, J. Perkins, C. J. Urch, *J. Chem. Soc. Perkin Trans. 2* **2001**, 651–669.
[21] E. A. Meyer, R. K. Castellano, F. Diederich, *Angew. Chem.* **2003**, *115*, 1244–1287; *Angew. Chem. Int. Ed.* **2003**, *42*, 1210–1250.
[22] M. Yoshizawa, J. Nakagawa, K. Kumazawa, M. Nagao, M. Kawano, T. Ozeki, M. Fujita, *Angew. Chem.* **2005**, *117*, 1844–1847; *Angew. Chem. Int. Ed.* **2005**, *44*, 1810–1813.
[23] S. Mirtschin, A. Slabon-Turski, R. Scopelliti, A. H. Velders, K. Severin, *J. Am. Chem. Soc.* **2010**, *132*, 14004–14005.
[24] R. Chakrabarty, P. S. Mukherjee, P. J. Stang, *Chem. Rev.* **2011**, *111*, 6810–6918.
[25] T. R. Cook, Y.-R. Zheng, P. J. Stang, *Chem. Rev.* **2013**, *113*, 734–777.
[26] M. M. J. Smulders, I. A. Riddell, C. Browne, J. R. Nitschke, *Chem. Soc. Rev.* **2013**, *42*, 1728–1754.
[27] T. Nakamura, H. Ube, M. Shionoya, *Chem. Lett.* **2013**, *42*, 328–334.
[28] N. Fujita, K. Biradha, M. Fujita, S. Sakamoto, K. Yamaguchi, *Angew. Chem.* **2001**, *113*, 1768–1771; *Angew. Chem. Int. Ed.* **2001**, *40*, 1718–1721.
[29] M. L. Merlau, M. del P. Mejia, S. T. Nguyen, J. T. Hupp, *Angew. Chem.* **2001**, *113*, 4369–4372; *Angew. Chem. Int. Ed.* **2001**, *40*, 4239–4242.

[30] E. Stulz, Y.-F. Ng, S. M. Scott, J. K. M. Sanders, *Chem. Commun.* **2002**, 524 – 525.
[31] R. Takahashi, Y. Kobuke, *J. Am. Chem. Soc.* **2003**, *125*, 2372 – 2373.
[32] J. Aimi, Y. Nagamine, A. Tsuda, A. Muranaka, M. Uchiyama, T. Aida, *Angew. Chem.* **2008**, *120*, 5231 – 5234; *Angew. Chem. Int. Ed.* **2008**, *47*, 5153 – 5156.
[33] A. K. Bar, R. Chakrabarty, G. Mostafa, P. S. Mukherjee, *Angew. Chem.* **2008**, *120*, 8583 – 8587; *Angew. Chem. Int. Ed.* **2008**, *47*, 8455 – 8459.
[34] W. Meng, B. Breiner, K. Rissanen, J. D. Thoburn, J. K. Clegg, J. R. Nitschke, *Angew. Chem.* **2011**, *123*, 3541 – 3545; *Angew. Chem. Int. Ed.* **2011**, *50*, 3479 – 3483.
[35] T. Nakamura, H. Ube, M. Shiro, M. Shionoya, *Angew. Chem.* **2013**, *125*, 748 – 751; *Angew. Chem. Int. Ed.* **2013**, *52*, 720 – 723.
[36] A review on four-coordinate, square-planar Ag^{I} complexes: A. G. Young, L. R. Hanton, *Coord. Chem. Rev.* **2008**, *252*, 1346 – 1386.
[37] For diversity in coordination geometries of Ag^{I} ions, see: M. C. Gimeno, A. Laguna in *Comprehensive Coordination Chemistry II: From Biology to Nanotechnology*, Vol. 6 (Ed.: D. E. Fenton), Elsevier, Amsterdam, **2004**, pp. 911 – 1145.
[38] C.-J. Fang, C.-Y. Duan, H. Mo, C. He, Q.-J. Meng, Y.-J. Liu, Y.-H. Mei, Z.-M. Wang, *Organometallics* **2001**, *20*, 2525 – 2532.
[39] D. A. Beauchamp, S. J. Loeb, *Chem. Commun.* **2002**, 2484 – 2485.
[40] B. Conerney, P. Jensen, P. E. Kruger, C. MacGloinn, *Chem. Commun.* **2003**, 1274 – 1275.
[41] E. C. Constable, C. E. Housecroft, B. M. Kariuki, C. B. Smith, *Aust. J. Chem.* **2006**, *59*, 30 – 33.

